Tracing Atlantic water transit time in the subarctic and Arctic Atlantic using ^{99}Tc-^{233}U-^{236}U

Lin, Gang; Qiao, Jixin; Steier, Peter; Danielsen, Magnús; Guðnason, Kjartan; Joensen, Hans Pauli; Stedmon, Colin A.

Published in:
Science of the Total Environment

Link to article, DOI:
10.1016/j.scitotenv.2022.158276

Publication date:
2022

Document Version
Publisher's PDF, also known as Version of record

Science of the Total Environment 851 (2022) 158276

Contents lists available at ScienceDirect

Science of the Total Environment

journal homepage: www.elsevier.com/locate/scitotenv

Tracing Atlantic water transit time in the subarctic and Arctic Atlantic using ^{99}Tc-^{233}U-^{236}U

Gang Lin [a], Jixin Qiao [a,*], Peter Steier [b], Magnús Danielsen [c], Kjartan Guðnason [d], Hans Pauli Joensen [e], Colin A. Stedmon [f]

[a] Department of Environmental and Resource Engineering, Technical University of Denmark, DK-4000 Roskilde, Denmark
[b] VERA Laboratory, Faculty of Physics, Isotope Physics, University of Vienna, Währinger Straße 17, A-1090 Vienna, Austria
[c] Marine and Freshwater Research Institute, Iceland
[d] Icelandic Radiation Safety Authority, Iceland
[e] University of the Faroe Islands, FO-110 Tórshavn, Faroe Islands
[f] National Institute of Aquatic Resources, Technical University of Denmark, Kemitorvet, 2800 Kgs. Lyngby, Denmark

HIGHLIGHTS

- New ^{99}Tc^{-233}U-^{236}U radiotracer approach to estimate Atlantic water transit time.
- Time-dependent ratios of ^{99}Tc and ^{236}U from reprocessing discharge applied.
- Reprocessing plants ^{236}U is isolated from global fallout using ^{233}U.
- Atlantic water transit times from Sellafield to Greenland coast are 16–22 years.

GRAPHICAL ABSTRACT

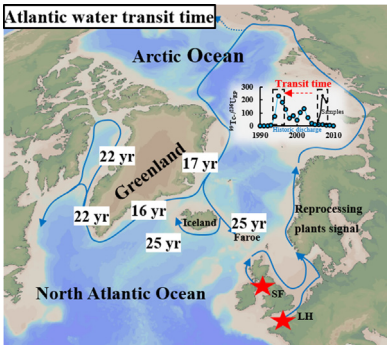

ARTICLE INFO

Editor: Jay Gan

Keywords:
^{99}Tc
^{233}U
^{236}U
Atlantic water
Transit time
Greenland-Iceland-Faroe Islands coast

ABSTRACT

The pathway and transport time of Atlantic water passing northern Europe can be traced via anthropogenic radioisotopes released from reprocessing of spent nuclear fuels at Sellafield (SF) and La Hague (LH). These reprocessing derived radioisotopes, with extremely low natural background, are source specific and unique fingerprints for Atlantic water. This study explores a new approach using ^{99}Tc-^{233}U-^{236}U tracer to estimate the transit time of Atlantic water in the coast of Greenland. We isolate the reprocessing plants (RP) signal of ^{236}U ($^{236}U_{RP}$) by incorporating ^{233}U measurements and combine this with ^{99}Tc which solely originates from RP, to estimate the transit time of Atlantic water circulating from Sellafield to the coast of Greenland-Iceland-Faroe Islands. Both being conservative radioisotopes, the temporal variation of ^{99}Tc/$^{236}U_{RP}$ ratio in Atlantic water is only influenced by their historic discharges from RP, thus ^{99}Tc/$^{236}U_{RP}$ can potentially be a robust tracer to track the transport of Atlantic water in the North Atlantic-Arctic region. Based on our observation data of ^{99}Tc-^{233}U-^{236}U in seawater and the proposed ^{99}Tc/$^{236}U_{RP}$ tracer approach, Atlantic water transit times were estimated to be 16–22, 25 and 25 years in the coast of Greenland, Iceland and Faroe Island, respectively. Our estimates from northeast Greenland coastal waters agree with earlier results (17–22 years). Therefore, this work provides an independent approach to estimate Atlantic water transit time with which to compare estimates from ocean modelling and other radiotracer approaches.

* Corresponding author.
E-mail address: jiqi@dtu.dk (J. Qiao).

http://dx.doi.org/10.1016/j.scitotenv.2022.158276
Received 20 May 2022; Received in revised form 18 August 2022; Accepted 21 August 2022
Available online 25 August 2022

1. Introduction

Atlantic water plays a key role in the Arctic climate due to the transport of entrained heat from lower latitudes (Muilwijk et al., 2018). Atlantic water enters the Arctic through the Fram Strait and Barents Sea, and exits along East Greenland coast. Variations in the properties and intensity of the Atlantic inflow influences sea-ice formation and melt, hereby effecting spatial and vertical distribution of heat and salt (and freshwater) in the region, which has a great potential to influence global circulation and climate (Polyakov et al., 2017; Halloran et al., 2020). Similarly, changes in circulation and stratification patterns have the potential to influence the marine food web, by altering nutrient supply (Hátún et al., 2017) and by supporting migration of species into new areas (Carscadden et al., 2013; Hátún et al., 2016).

Anthropogenic radionuclides (such as ^{90}Sr, ^{137}Cs, ^{99}Tc, ^{129}I and ^{236}U) emitted from the European reprocessing plants (RP) at Sellafield (SF) and La Hague (LH) are useful tracers for Atlantic water in the Arctic Ocean (Aarkrog et al., 1987; Dahlgaard, 1994; Hou et al., 2000; Smith et al., 2011, 2021; Casacuberta et al., 2014, 2018; Wefing et al., 2019, 2021), as Arctic seawater has contributions from various sources (Atlantic water, Pacific water and freshwater), and only Atlantic water is tagged with RP derived radioisotopes signals. ^{90}Sr and ^{137}Cs are good examples of RP specific marine tracers (Dahlgaard, 1995a; Smith et al., 2011; Rozmaric et al., 2022) as both were released in significant amounts during 1970s – 1980s. In this light the RP signal of ^{90}Sr and ^{137}Cs from SF can be used to estimate Atlantic water transit time in the Arctic and subpolar region (Dahlgaard, 1995a; OSPAR, 2019). However, their application is limited by their relatively short half-lives (^{90}Sr t½ = 28.8 yr and ^{137}Cs t½ = 30.2 yr). In contrast, long-lived radioisotopes such as ^{233}U, ^{236}U, ^{129}I and ^{99}Tc, can trace ocean circulation over longer time scales. In addition, ^{137}Cs is readily attached to particles, thereby scavenged from water columns into sediments (distribution coefficient (K_d) for ^{137}Cs between sediment and seawater is 2000. This also urges us to explore other more conservative radioisotopes to trace water mass movement, such as ^{99}Tc (K_d = 100), ^{129}I (K_d = 200) and U isotopes (K_d = 500) (International Atomic Energy Agency IAEA, 2004).

In recent years, ^{236}U (t½ = 23.4 Myr) has been recognized as a powerful Atlantic water tracer, especially when combing with another long-lived RP derived tracer ^{129}I (t½ = 15.7 Myr) (Christl et al., 2012; Casacuberta et al., 2014, 2016, 2018; Wefing et al., 2019, 2021). Several studies demonstrated the successful application of ^{236}U—^{129}I tracer pair to identify and trace the flow of water from the North Atlantic into the Arctic Ocean. For instance, the transit times of Atlantic water in the Arctic surface layer from the entrance of the Arctic Ocean (74°N, 19°E) have been reported in the range of 3–12 years in the Nansen Basin, 9–16 years in the Amundsen Basin, 2–14 years in the Makarov Basin, 14–20 years in the Canada Basin and 12–17 years in the Fram Strait via the combination of ^{129}I and ^{236}U as tracers (Wefing et al., 2021).

Anthropogenic ^{236}U is mainly derived from RP (115–200 kg, with majority from SF) and global fallout (GF, 900–1400 kg) (Steier et al., 2008; Sakaguchi et al., 2009, 2012). The reconstructed discharge of ^{236}U from RP showed a gradually decreasing trend since the 1970s, varying within 1–31.3 kg/yr at SF during 1971–2018, and 0.2–2.1 kg/yr at LH during 1967–2017 (Fig. S1) (Castrillejo et al., 2020). Due to rapid atmospheric mixing, GF-derived ^{236}U is a ubiquitous source affecting all regions in the world with a gradually decreasing deposition after the 1970s (Fig. S2) (Christl et al., 2015). Previous studies using ^{236}U as an oceanic tracer have assumed GF ^{236}U contribution to be constant after 1990 (Wefing et al., 2019, 2021) and this may introduce uncertainties in the transit time estimation.

The development of advanced accelerator mass spectrometry (AMS) technique allows the quantification of another long-lived uranium isotope, ^{233}U (t½ = 0.159 Ma) in environmental samples. Anthropogenic ^{233}U is primarily produced through the ^{235}U (n,3n) ^{233}U reaction by fast neutrons or directly by ^{233}U-fueled devices in thermonuclear explosions. The ^{233}U production in nuclear power reactors or reprocessing plants is negligible (Hain et al., 2020). Therefore, the ^{233}U/^{236}U ratios in the RP and GF endmembers are very different, and the coupling of ^{233}U with ^{236}U signature presents the possibility to distinguish between the two different ^{236}U source terms, RP and GF through a linear mixing model (detailed explanation see Section 2.7, Hain et al., 2020; Qiao et al., 2020a). Although previous study shows that sediment in the shallow European Shelf Seas acts as minor sinks of ^{236}U (Periáñez et al., 2018), isotopic fractionate between ^{233}U and ^{236}U is not expected to occur as any alternations in biogeochemical behavior will equally affect all the isotopes of uranium, highlighting the robustness of ^{233}U—^{236}U pair in oceanic tracer studies.

Radioisotopes from the two RPs in Europe have been released at different concentrations in different years, and this can be used to trace Atlantic water transit times. Combining estimates of RP-derived ^{236}U with another conservative RP-derived radioisotope with a different discharge profile, enables one to use their ratios to determine Atlantic water transit time. This is because the ratios of RP-derived isotopes in Atlantic water is only dependent on the RP discharge histories and not affected by the dilution of other waters along the transport. This has been demonstrated earlier with coupled measurements of ^{129}I and ^{236}U (Wefing et al., 2021). However, ^{129}I is primarily released from LH, whereas ^{236}U is predominantly released from SF (Fig. S1). Different transport passage and transit times of Atlantic water to Arctic from LH compared with from SF may complicate the application. It is therefore, relevant to consider other source specific radioisotopes with which to compare current estimates of Atlantic water transit times.

Since the early 1980s, the long-lived and conservative ^{99}Tc (t½ = 0.211 Myr) has been applied to trace Atlantic water transport in the Nordic seas and Arctic Ocean (Aarkrog et al., 1987; Kershaw et al., 1999; Karcher et al., 2004). ^{99}Tc has a dominant source (> 90 %) from RP (cumulative emission of 1720 TBq from SF and 154 TBq from LH, Fig. S1) (Shi et al., 2012) and only a minor contribution from GF (140 TBq) and other sources such as nuclear power plants, medical applications of ^{99m}Tc and nuclear accidents (e.g., Chernobyl (ca. 0.75 TBq ^{99}Tc) and Fukushima) (Shi et al., 2012). The discharge histories of ^{99}Tc from RP are characterized by two peak-release periods in 1970–1980 and 1994–2003, respectively, both were related to the operation of SF (Fig. S1). Therefore, the combination of ^{99}Tc and RP-derived ^{236}U has a potential to assess transport time scales of Atlantic water in the Arctic Ocean while eliminating uncertainties from GF ^{236}U and avoiding the reconstruction of combined RP ^{236}U input function from SF and LH contributions based on certain assumptions for the water mixing in the North Sea and Norwegian Sea.

In this study, we aim to apply a ^{99}Tc-^{233}U-^{236}U approach to estimate the transit time of Atlantic water across the Nordic Seas to the coast of Greenland, Iceland and Faroe Islands. The approach isolated RP-derived ^{236}U signal through ^{233}U measurement avoids potential interference from the GF ^{236}U signal, which is supplied in Pacific water exiting the Arctic Ocean and in glacial and sea-ice meltwater. In addition, some ^{137}Cs and ^{90}Sr seawater data obtained from an earlier marine radioactivity monitoring program were compiled to support our interpretation on the potential current transport in the study area.

2. Material and methods

2.1. Study area and sampling

The study area includes the coastal waters of Greenland, southern Iceland and the Faroe Islands (Fig. 1A). The eastern and western Greenland coastal waters are dominated by the southwards flowing East Greenland Current and northward flowing West Greenland Current, respectively. East and West Greenland Currents mainly consist of outflowing Polar Surface Water and returning Atlantic waters. In the southeast of the region, Atlantic mode water directly transports waters from the North Atlantic to the southern coast of Iceland and Faroe Islands (Daniault et al., 2016). One branch of direct Atlantic water moves westward to the southeastern Greenland coast, while another branch water continuously transports to the Norwegian Sea (Daniault et al., 2016).

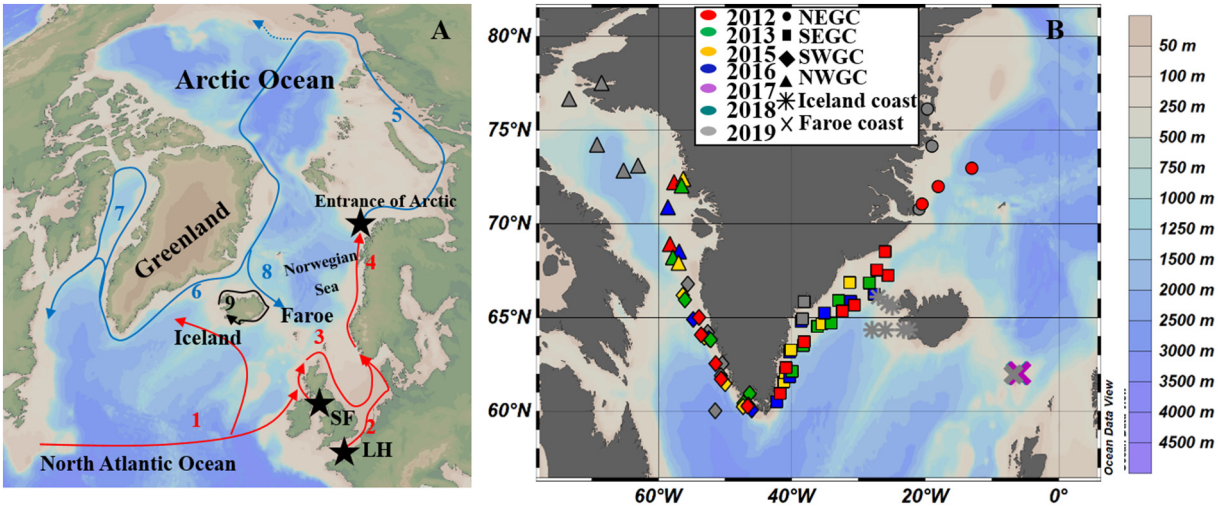

Fig. 1. The selected surface currents transporting RP signal in the Arctic-North Atlantic region (A). The sites of sampling location (B). Currents are labelled by the number: 1. North Atlantic Current; 2. La Hague branch water; 3.Sellafield branch water; 4. Norwegian Coastal Current; 5. Norwegian Coastal Current in the Arctic Ocean; 6. East Greenland Current; 7. West Greenland Current; 8. A branch of East Greenland Current to the northern coast of Iceland (Casanova-Masjoan et al., 2020); 9. The coastal current of Iceland. Red lines refer to the transport of surface Atlantic water in the North Atlantic Ocean, and blue lines refer to the transport of surface Atlantic water in the Arctic Ocean and Greenland coast. NEGC: north-eastern Greenland coast; SEGC: south-eastern Greenland coast; SWGC: south-western Greenland coast; NWGC: north-western Greenland coast.

Sampling was carried out in 1991–1999 and 2012–2019 through the collaboration of Technical University of Denmark, Marine and Freshwater Research Institute, Iceland, and University of Faroe Islands. In total of 96 seawater samples were collected at 0–10 m depth along the coasts of Greenland-Iceland-Faroe in 2012–2019 (Fig. 1B), and processed for ^{99}Tc, ^{233}U, ^{236}U and ^{238}U analysis. Twelve additional samples were collected earlier in Faroe Islands coastal waters (1991–1999), and prepared for ^{90}Sr and ^{137}Cs measurement within a marine radioactivity monitoring program at Technical University of Denmark (DTU). ^{233}U–^{236}U-^{238}U measurements from Greenland coastal waters during 2012–2016 have been published earlier (Qiao et al., 2020a). More detailed sample information is provided in Table S1 (Supporting Information).

2.2. Standards and materials

Uranium standard solution (1.000 g/L in 2 mol/L HNO_3) was purchased from NIST (Gaithersburg, MD) and used as a standard for ^{238}U measurement after dilution with 0.5 mol/L HNO_3. ^{99m}Tc tracer was obtained from 2 to 4 GBq commercial ^{99}Mo-^{99m}Tc generators (Amersham, UK) and was purified using alumina cartridges. All reagents used in the experiment were of analytical reagent grade and prepared using ultra-pure water (18 MΩ·cm). UTEVA resin (100–150 μm particle size) was purchased from Triskem International, Bruz, France and packed in 2-mL Econo-Columns (0.7 cm i.d. × 5 cm length, Bio-Rad Laboratories Inc., Hercules, CA) for the chemical purification of uranium isotopes. Anion exchange chromatography (AG 1 × 4 resin, 100–150 mesh particle size, Bio-Rad Laboratory, USA) was used to concentrate ^{99}Tc from seawater samples.

2.3. Determination of ^{99}Tc

The determination of ^{99}Tc in seawater is based on the procedure reported earlier (Chen et al., 1994), which is briefly described below. After spiking with ^{99m}Tc as a yield monitor, each seawater (ca. 200 L) was preconcentrated using anion exchange chromatography (AG 1 × 4 resin). ^{99}Tc was further purified using a second anion exchange chromatographic separation followed by solvent extraction (5 % triisooctylamine (TIOA)-xylene). After the source preparation using electrodeposition, the activity of ^{99}Tc was measured using an anticoincidence gas flow Geiger-Müller (GM) counter (Risø, Denmark). The chemical yields of technetium for the whole procedure were measured by counting the ^{99m}Tc tracer using a NaI detector.

2.4. Determination of ^{233}U, ^{236}U and ^{238}U

The radiochemical separation of uranium isotopes from seawater samples was performed according to earlier studies (Qiao et al., 2015; Lin et al., 2021a). To 5–10 L of filtered seawater, 14 M HNO_3 was added to adjust pH = 2 to release uranium ion from the uranyl carbonate complexes. 500–1000 mg Fe^{3+} (0.05 g/mL purified $FeCl_3$ solution using UTEVA® resin) was added, and the sample was vigorously stirred (10 min) with air to expel the dissolved CO_2. pH value was adjusted to 8–9 through 25 % $NH_3{\cdot}H_2O$ solution for co-precipitating iron hydroxides with uranium. The sample was kept still for 1–2 h to allow the iron hydroxide co-precipitate to settle down. The supernatant was decanted and the remaining sludge was centrifuged at 3000 rpm for 10 min. The obtained precipitate was dissolved with 14 M HNO_3 and then diluted to 3 M HNO_3. A 2-mL UTEVA® resin column was preconditioned with 20 mL of 3 M HNO_3 and used for the chromatographic separation of uranium. The column was rinsed with 40 mL of 3 M HNO_3 and 20 mL of 6 M HCl, respectively. Uranium was eluted by 10 mL of 0.025 M HCl. 2 mg of Fe^{3+} was added to the eluate to form iron hydroxide co-precipitate after adjusting the pH to 8–9 with 25 % $NH_3{\cdot}H_2O$. The precipitate was separated via centrifugation, dried in an oven at 90 °C for 4 h, and combusted in a muffle furnace at 800 °C for 12 h. After cooling, the combusted sample was pressed into an aluminum sputter target holder for ^{233}U/^{238}U and ^{236}U/^{238}U measurement. The measurement was carried out by accelerate mass spectrometry (AMS) at the Vienna Environmental Research Accelerator (VERA) facility, in the University of Vienna (Steier et al., 2010; Hain et al., 2020).

To monitor the laboratory background (Lin et al., 2021a), one procedure blank was processed with the same procedure for every seven seawater samples. All chemical separations were carried out in a laminar flow bench with the use of purified chemicals and carefully cleaned (with acid boiling) glassware for reducing the background level. The ^{233}U (0) and ^{236}U (< 0.1) count rates of all blank samples were significantly low (< 2 %) compared to those in seawater samples. The uncertainties of ^{233}U and ^{236}U were expanded uncertainties (with a coverage factor k = 1) including the measurement uncertainties of ^{238}U contents, ^{233}U/^{238}U and ^{236}U/^{238}U in the eluates of seawater and blank samples. The detailed description was reported in the previous work (Lin et al., 2021a).

^{238}U concentration in the raw seawater and the U eluate from UTEVA column was diluted with 0.5 M HNO_3 and measured by the inductively coupled plasma mass spectrometry (ICP-MS) (ICP-QQQ 8800, Agilent) using indium or bismuth as an internal standard (Qiao and Xu, 2018).

2.5. Determination of ^{90}Sr

The detailed procedure of ^{90}Sr in seawater is reported in a previous study (Chen et al., 2002), and it is briefly described below. The ^{85}Sr tracer and $SrCl_2{\cdot}H_2O$ carrier were added into 45 L seawater with stirring for 10 min. NaOH was added to adjust pH = 8–10. After boiling, 2 M $(NH_4)_2CO_3$ was added with stirring to form $SrCO_3/CaCO_3$ precipitation. After siphoning off the supernatant, the $SrCO_3/CaCO_3$ precipitate was dissolved in 4 M HNO_3 followed by addition of Fe^{3+}. 6 M NaOH was then added to a concentration of 0.5 M NaOH to separate Ca (as $Ca(OH)_2$) from Sr. After centrifuging, 0.2 M NaOH was used to wash the $Ca(OH)_2$ precipitate. The supernatant and washes were combined and heated at 250 °C for 1 h. Na_2CO_3 was added to precipitate Sr as $SrCO_3$ which was thereafter dissolved with 8 M HNO_3. The $Ca(OH)_2$ and $SrCO_3$ precipitation were repeated to ensure a sufficient remove of Ca. The finally obtained $SrCO_3$ precipitate was dissolved with 6 M HNO_3, and after addition of $FeCl_3$, adjusted to pH 10 with NaOH. The supernatant was added with Y^{3+} carrier and Ba^{2+} carrier after centrifuging. After waiting (approximately 3 weeks) for the ingrowth of ^{90}Y (daughter radionuclide of ^{90}Sr), Sr and Ba in the sample solution were separated from Y via $BaSO_4$ and $SrSO_4$ precipitation. Y was finally prepared as $Y_2(C_2O_4)_3$ for the ^{90}Y radioactivity measurement using an anti-coincident gas flow GM counter (Risø, Denmark). The ^{90}Sr radioactivity concentration in the sample was thereby obtained via ^{90}Y based on the decay equilibrium.

2.6. Determination of ^{137}Cs

^{137}Cs determination in seawater is based on a previous report (Qiao et al., 2020b). To 45 L of filtered seawater, 14 M HNO_3 was added to acidify seawater to pH = 2. 30 mg of Cs carrier (CsCl) and 50 mg of ammonium molybdophosphate (AMP) were added with stirring for 1 h. After allowing the AMP to settle overnight and discarding the supernatant, the slurry was filtered and dried in an oven under 105 °C. The dried AMP powder was measured for ^{137}Cs by gamma spectrometry using high-purity germanium detectors. The Cs chemical yield was calculated through weighing the AMP powder (Eq. (1)) and results indicated high recovery (> 95 %).

$$Yield_{Cs} = \frac{Final\ weight_{AMP\ powder}}{Initial\ weight_{AMP\ powder}} \times 100\% \quad (1)$$

2.7. Estimation of reprocessing plants contribution to ^{236}U

The contributions of RP and GF in ^{236}U can be distinguished through the atomic ratio of $^{233}U/^{236}U$ and the following Eqs. (2)–(3) resolved from a two-endmember mixing algorithm (Qiao et al., 2020a).

$$P_{RP} = \frac{R_{GF} - R_S}{R_{GF} - R_{RP}} \quad (2)$$

$$^{236}U_{RP} = {}^{236}U_S \times P_{RP} \quad (3)$$

where P_{RP} is the fraction of RP-derived ^{236}U in the seawater sample (Table S1); R_S is the measured $^{233}U/^{236}U$ atomic ratio in the seawater sample; R_{RP} is the $^{233}U/^{236}U$ atomic ratio in RP endmember (1×10^{-7}) (HELCOM MORS Discharge database, 2020); R_{GF} is the $^{233}U/^{236}U$ atomic ratio in GF endmember ($1.4 \pm 0.15 \times 10^{-2}$) (Hain et al., 2020); $^{236}U_{RP}$ is the RP-derived ^{236}U concentration in the seawater sample, $^{236}U_S$ is the measured ^{236}U concentration in the seawater sample.

2.8. Estimation of Atlantic water transit times based on $^{99}Tc/^{236}U_{RP}$ ratios

The temporal change of $^{99}Tc/^{236}U_{RP}$ ratios is established based on the ^{99}Tc and ^{236}U annual discharges from SF and LH, considering a 2-year lag time for the SF release to be mixed with LH release during transport northwards along the Norwegian coast (Fig. 2). The ^{236}U discharges from SF and LH were based on the data reported by Castrillejo et al. (2020). The discharges of ^{99}Tc from SF and LH were compiled from several earlier works (Jackson, 2000; OSPAR, 2019; Shi et al., 2012). Based on our hypothesis that $^{99}Tc/^{236}U_{RP}$ ratio tagged in the Atlantic water is only dependent on their release pattern from RP, by comparing the measured $^{99}Tc/^{236}U_{RP}$ in seawater samples with the established temporal variation of $^{99}Tc/^{236}U_{RP}$ in the RP release, we could allocate the source year of the Atlantic water. However, the temporal variation of $^{99}Tc/^{236}U_{RP}$ in RP release has several peaks in 1993–2005 (Fig. 2). To constrain the source year, a time series of $^{99}Tc/^{236}U_{RP}$ measurements from the same region can be used to compare with the temporal trend of $^{99}Tc/^{236}U_{RP}$ in the RP discharge (Fig. 2).

3. Results

3.1. The temporal and spatial distribution of radioisotopes in the coastal waters of Greenland, Iceland and Faroe Islands

To facilitate the data interpretation, we divided the study region into four areas around Greenland: the north-eastern Greenland coast (NEGC), the south-eastern Greenland coast (SEGC), the south-western Greenland coast (SWGC) and the north-western Greenland coast (NWGC); and Icelandic and Faroe Island coastal waters (Fig. 3, Table 1). ^{99}Tc concentrations in surface waters ranged from 0.01 to 0.94 Bq/m^3 during 2012–2019 (Fig. 3A). Highest values were detected in the SEGC in 2013 and NEGC in 2019 while the lowest concentrations were measured in NWGC in 2012 and Faeroe Island waters in 2019. The range of ^{236}U concentrations (8.98–120.27 $\times 10^6$ atom/L) from the coastal waters of Greenland and Iceland in 2019 and Faroe Islands waters in 2016–2019 were comparable with reported earlier results (7.38–128.60 $\times 10^6$ atom/L) for Greenlandic waters in 2012–2016, but a narrower range of ^{233}U (4.10–23.66 $\times 10^4$ atom/L) was reported for the earlier study (^{233}U concentrations: 2.64–45.70 $\times 10^4$ atom/L) (Fig. 3B and C) (Qiao et al., 2020a). And the range of $^{233}U/^{236}U$ ratios obtained in this work are 0.05–1.71 $\times 10^{-2}$ (Fig. 3D). Based on the Eq. (2), the RP fractions of ^{236}U can be calculated and were for Greenland samples (0.18–0.92 during 2012–2019), Iceland (0.24–0.64 in 2019) and Faroe Islands (0–0.96 during 2016–2019). For some samples, the ratios of $^{233}U/^{236}U$ are even higher than the GF endmember value ($1.40 \pm 0.15 \times 10^{-2}$). This may be induced by either uncertainties from measurement or the spatiotemporal variation of $^{233}U/^{236}U$ ratios in GF signals as observed in other studies (Qiao et al., 2022; Lin et al., 2021b). The ratio of $^{233}U/^{236}U$ in GF endmember was estimated from corals and sediments in the low-mid latitudes (Hain et al., 2020), and the nuclear weapons testing in the high latitude (i.e. Novaya Zemlya Island in the Arctic) may also potentially contribute to ^{233}U budget to the Arctic Ocean (Chamizo et al., 2022), resulting in such variability of $^{233}U/^{236}U$ ratios in different latitudes belts.

3.2. The temporal and spatial trends in $^{99}Tc/^{236}U_{RP}$ atomic ratios

$^{99}Tc/^{236}U_{RP}$ atomic ratios ranged from 2 to 525 during 2012–2019 in Greenland coastal waters. (Fig. 3E, Table 2). The highest average value was obtained in NEGC in 2019, and the lowest values were seen in NWGC in the years of 2012. In general, $^{99}Tc/^{236}U_{RP}$ atomic ratios show a gradual decrease trend from NEGC to NWGC in the same year during 2012–2019. In contrast, $^{99}Tc/^{236}U_{RP}$ ratios in Icelandic and Faroe Islands coastal waters were much less variable, ranging between 26 and 94 and 2–139, respectively (Fig. 3E, Table 2).

It is worth noting that there is extremely low $^{99}Tc/^{236}U_{RP}$ atomic ratio in SEGC (2013, 2 ± 1) and Faroe Island (2019, 2 ± 1) due to the

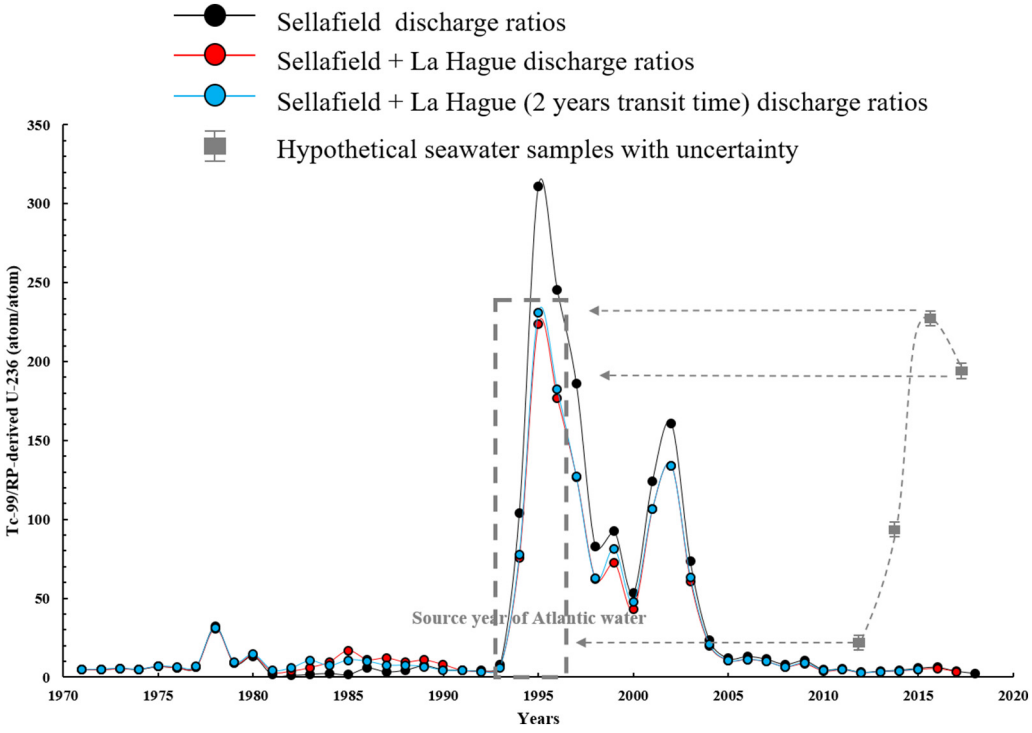

Fig. 2. An example of the approach to estimate Atlantic water source year by comparing times series $^{99}Tc/^{236}U_{RP}$ atomic ratios in samples from a specific region with the temporal changes of ratios in the RP discharge from Sellafield (black line), Sellafield and La Hague (red line), Sellafield and La Hague (with 2 year delay to account for transport time from SF to LH) (light blue line) discharge ratios. The year in the x-axis corresponds to the year of radioactive release from Sellafield. In this figure, the $^{99}Tc/^{236}U_{RP}$ atomic ratios in seawater samples are hypothetical data for better explanation.

significantly high concentration of $^{236}U_{RP}$ (117.7 ± 15.8 and 115.9 ± 7.9 × 10^6 atom/L, respectively). This extremely high concentration of $^{236}U_{RP}$ may be derived from another transport pathway (see Section 4.2 in detail), thus was not included in the initial estimation for Atlantic water transit time.

(data marked with * are from Qiao et al., 2020a, data marked with # are presented as value ± uncertainty as only a single sample was obtained in the corresponding region)

3.3. The temporal distribution of ^{90}Sr and ^{137}Cs in the coastal water of Faroe Islands

The continuous observation of ^{90}Sr and ^{137}Cs was performed in same location of Faroe Islands coast during 1991–1999. ^{90}Sr concentrations in surface waters varied within 0.55–1.44 Bq/m^3, while ^{137}Cs concentrations ranged from 1.47 to 9.96 Bq/m^3 (Table S1). The lowest concentration of ^{90}Sr (0.55 ± 0.0003 Bq/m^3) was measured in 1992, and the highest

Table 1
^{99}Tc, ^{233}U and ^{236}U average concentrations and $^{233}U/^{236}U$ average ratios with standard deviations (SD) or uncertainties in the coastal water of Greenland, Iceland and Faroe Islands ("average" refers to arithmetic mean).

Station	^{99}Tc (Bq/m^3)	^{233}U (× 10^4 atom/L)	^{236}U (× 10^6 atom/L)	$^{233}U/^{236}U$ (× 10^{-2})
The NEGC in 2012	0.14 ± 0.03 (*n* = 3)	3.8 ± 1.2*#	11.1 ± 3.0* (n = 3)	0.42 ± 0.14*#
The SEGC in 2012	0.13 ± 0.06 (*n* = 8)	9.3 ± 2.5*#	16.3 ± 7.2* (n = 8)	0.32 ± 0.09*#
The SWGC in 2012	0.13 ± 0.07 (*n* = 5)	5.3 ± 1.0* (n = 5)	26.5 ± 4.5* (n = 5)	0.21 ± 0.07* (n = 5)
The NWGC in 2012	0.02 ± 0.01 (*n* = 2)	7.2 ± 3.4* (*n* = 2)	22.1 ± 1.6* (*n* = 2)	0.34 ± 0.18* (*n* = 2)
The SEGC in 2013	0.25 ± 0.35 (*n* = 7)	15.8 ± 14.4* (n = 7)	48.0 ± 39.7* (n = 7)	0.42 ± 0.38* (n = 7)
The SWGC in 2013	0.14 ± 0.06 (n = 5)	7.7 ± 3.8* (n = 5)	29.8 ± 11.1* (n = 5)	0.26 ± 0.05* (n = 5)
The NWGC in 2013	0.10 ± 0.02 (*n* = 2)	13.6 ± 1.2* (n = 2)	26.2 ± 1.7* (n = 2)	0.52 ± 0.01* (n = 2)
The SEGC in 2015	0.09 ± 0.04 (*n* = 6)	9.0 ± 1.9* (n = 6)	18.5 ± 4.9* (n = 6)	0.50 ± 0.09* (n = 6)
The SWGC in 2015	0.10 ± 0.03 (*n* = 4)	9.0 ± 1.2* (*n* = 4)	25.7 ± 6.6* (n = 4)	0.37 ± 0.12* (n = 4)
The NWGC in 2015	0.10 ± 0.02 (*n* = 2)	6.5 ± 1.4* (n = 2)	22.2 ± 4.6* (*n* = 2)	0.29 ± 0.00* (n = 2)
The SEGC in 2016	0.12 ± 0.09 (n = 6)	4.5 ± 1.4* (n = 6)	13.9 ± 3.3* (*n* = 7)	0.33 ± 0.05* (n = 6)
The SWGC in 2016	0.12 ± 0.06 (*n* = 4)	9.5 ± 2.8* (*n* = 4)	15.5 ± 4.0* (n = 4)	0.61 ± 0.06* (n = 4)
The NWGC in 2016	0.08 ± 0.00 (n = 2)	7.7 ± 4.8* (n = 2)	16.2 ± 5.8* (n = 2)	0.45 ± 0.13* (n = 2)
The NEGC in 2019	0.17 ± 0.14 (n = 4)	11.0 ± 1.5 (n = 4)	15.5 ± 1.7 (n = 4)	0.71 ± 0.09 (n = 4)
The SEGC in 2019	0.07 ± 0.00#	8.2 ± 0.1 (n = 2)	13.3 ± 3.7 (n = 2)	0.64 ± 0.17 (n = 2)
The SWGC in 2019	0.08 ± 0.01 (n = 6)	9.0 ± 1.7 (n = 7)	14.6 ± 1.3 (n = 7)	0.62 ± 0.11 (n = 7)
The NWGC in 2019	0.07 ± 0.04 (n = 4)	9.3 ± 1.9 (*n* = 5)	15.7 ± 1.6 (n = 5)	0.59 ± 0.11 (n = 5)
Iceland in 2019	0.05 ± 0.05 (n = 2)	8.4 ± 1.7 (*n* = 9)	11.1 ± 2.4 (n = 9)	0.79 ± 0.19 (n = 9)
Faroe island in 2016		4.1 ± 1.9#	11.7 ± 1.3#	0.35 ± 0.17#
Faroe island in 2017	0.04 ± 0.02 (n = 4)	11.4 ± 2.0 (n = 2)	21.5 ± 12.4 (*n* = 3)	0.49 ± 0.19 (n = 2)
Faroe island in 2018	0.04 ± 0.00#	15.4 ± 5.8 (n = 4)	16.2 ± 6.6 (n = 4)	1.07 ± 0.54 (n = 4)
Faroe island in 2019	0.02 ± 0.01 (n = 4)	7.3 ± 2.5 (n = 4)	37.4 ± 55.3 (n = 4)	0.60 ± 0.44 (n = 4)

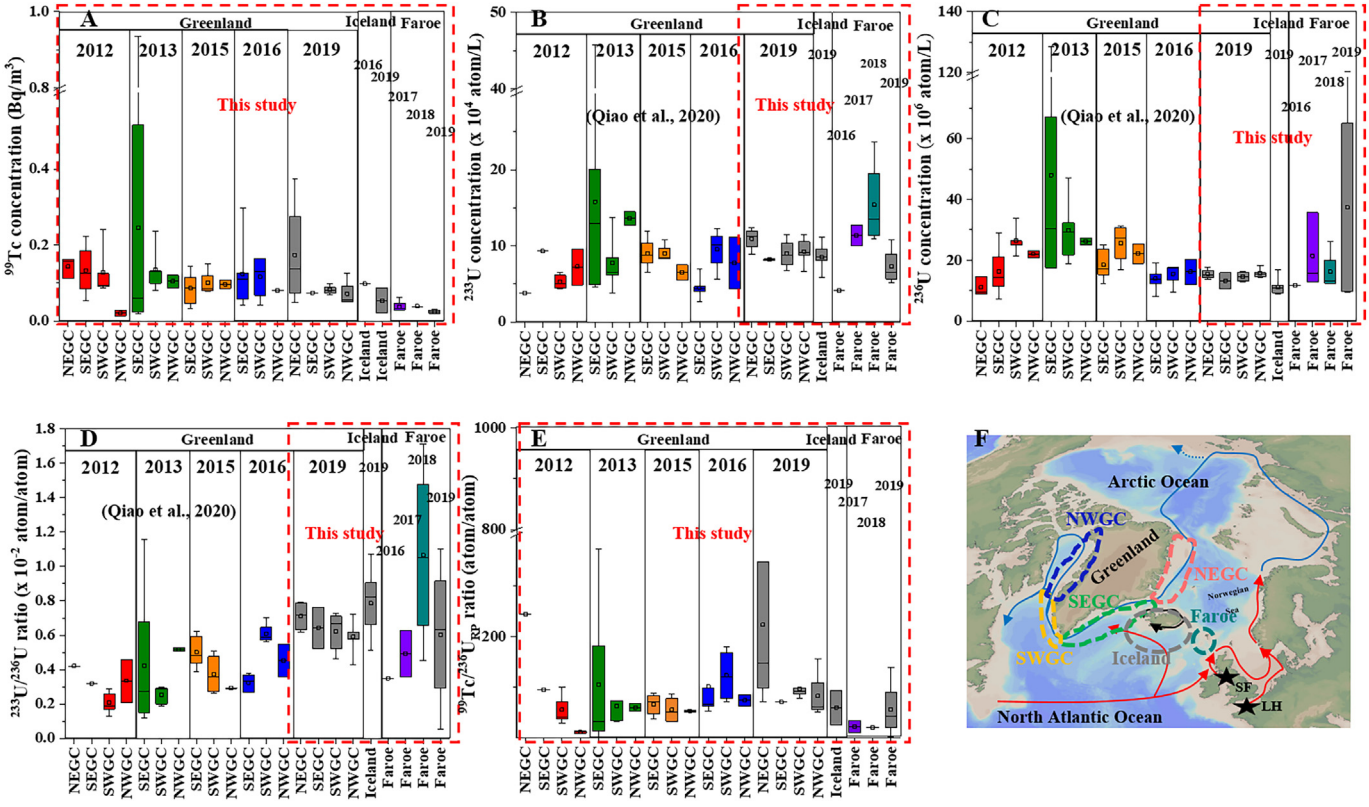

Fig. 3. The boxplot distributions of ^{99}Tc (A), ^{233}U (B) and ^{236}U (C) concentrations, ^{233}U/^{236}U atomic ratio (D), and ^{99}Tc/$^{236}U_{RP}$ atomic ratio (E) in coastal waters of Greenland, Iceland and Faroe Islands during 2012–2019, and the definition of the different areas in the study region (F). NEGC: north-eastern Greenland coast; SEGC: south-eastern Greenland coast; SWGC: south-western Greenland coast; NWGC: north-western Greenland coast. Data from Qiao et al. (2020a) are shown together with the results from this study.

value of ^{137}Cs (9.96 ± 0.43 Bq/m^3) was detected in 1997. The ^{137}Cs/^{90}Sr activity ratios were significantly higher in 1992 (4.36 ± 0.76) and 1997 (6.92 ± 0.34), compared to the other years where it remained between 1.03 and 2.21.

4. Discussion

4.1. Constraining the transit time of Atlantic water in Greenland-Iceland-Faroe Island coastal water using ^{99}Tc/$^{236}U_{RP}$ atomic ratio

Greenland coastal surface seawater is dominated by the outflowing Polar Surface Water entraining RP signal from the Norwegian Coastal Current (NCC) (Fig. 1) (Qiao et al., 2020a; Wefing et al., 2019, 2021). The use of discharge data from SF and LH enables a straightforward construction of the temporal variation of ^{99}Tc/$^{236}U_{RP}$ atomic ratio in the Atlantic water. Previous studies have reconstructed the input function in Atlantic water entering the Arctic Ocean by assuming a constant marine mixing proportion Casacuberta et al. (2018), which may introduce uncertainty in estimating transit time. However, the approach applied here is an attempt to circumnavigate this.

Based on the ^{236}U and ^{99}Tc historical data from SF and LH (Fig. S1), we calculated the temporal evolution of ^{99}Tc/$^{236}U_{RP}$ atomic ratio under three different scenarios: i) considering SF as the sole source of discharge; ii) considering both SF and LH contribute to discharge; and iii), considering both but with a 2-year transit time for SF to mix with LH discharge. For this latter scenario the discharge from SF for a given year was combined with the LH

Table 2
The estimation of Atlantic water transit time from Sellafield with ^{99}Tc/$^{236}U_{RP}$ average ratios and standard deviations (SD) or uncertainties in Greenland-Iceland-Faroe Islands coastal seawater.

Region	^{99}Tc/$^{236}U_{RP}$ average ratio in 2012	^{99}Tc/$^{236}U_{RP}$ average ratio in 2013	^{99}Tc/$^{236}U_{RP}$ average ratio in 2015	^{99}Tc/$^{236}U_{RP}$ average ratio in 2016	^{99}Tc/$^{236}U_{RP}$ average ratio in 2017	^{99}Tc/$^{236}U_{RP}$ average ratio in 2018	^{99}Tc/$^{236}U_{RP}$ average ratio in 2019	Transit time of Atlantic water (year)	Uncertainty of transit time (year)
Northeast Greenland coast (NEGC)	244 ± 61#						223 ± 205	17	
Southeast Greenland coast (SEGC)	95 ± 20#	122 ± 140 (105 ± 135)	66 ± 20	102 ± 72			71 ± 12#	16	±2
Southwest Greenland coast (SWGC)	56 ± 29	63 ± 46	56 ± 27	123 ± 53			97 ± 20	22	±2
Northwest Greenland coast (NWGC)	12 ± 3	60 ± 10	53 ± 2	74 ± 16			82 ± 49	22	±2
Iceland coast (IC)							60 ± 48	25	
Faroe Island coast (FIC)					22 ± 17	21 ± 3#	74 ± 20 (56 ± 59)	25	

Data marked with # show uncertainty due to only one data this year; data in parentheses contained the abnormal values with unexpected 236U concentrations.

discharge from two years later to account for transit between sites. Two year lag was chosen as previous work has showed that the transit times from SF and LH to the Arctic entrance were 5 and 3 years, respectively (Casacuberta et al., 2018). Fig. 2 shows how these scenarios influence the calculated temporal trend in $^{99}Tc/^{236}U_{RP}$ atomic ratios in the discharges. The ratios are comparable across these three scenarios, with two notable peaks in 1993–2000 and 2000–2005, respectively. Comparison of $^{99}Tc/^{236}U_{RP}$ atomic ratio for each sample with that reconstructed from the RP discharge allows us to constrain the source year, and the transit time of Atlantic water is estimated by aligning the time series of measurements to the discharge histories (Fig. 4).

The RP signal from SF and LH partly mixes in the North Sea and moves northward to the Arctic along the Norwegian coast (Fig. 1) (Christl et al., 2017; Casacuberta et al., 2018). The Norwegian Coastal Current carries RP signal onwards to the Barents Sea overflow and towards the Siberian shelf, whereafter it moves into the central Arctic Ocean along the Lomonosov ridge (Casacuberta et al., 2018). It dominates the RP signal input in surface seawater of the Arctic Ocean and outflows along the eastern Greenland coast (Wefing et al., 2021; Qiao et al., 2020a). Pacific water and freshwater, in contrast, carry a GF signal and also contribute to the outflow along the eastern Greenland coast.

Due to the westward water transport pathway from the northeastern Greenland coast to the northwestern Greenland coast, the samples in NEGC in same sampling years should be younger than those in other regions (namely, NEGC < SEGC < SWGC < NWGC) and this is indeed the case (Fig. 4). However, no significant statistical correlation was observed when using the annually-varied RP discharge ratios to align with our time-series observation. Instead correlations between the measurements and 3-year, 5-year and 7-year running averages of $^{99}Tc/^{236}U_{RP}$ ratios from the RP release were tested. The best correlation was obtained when using the 5-year running (i.e., the release year ±2 years) average of $^{99}Tc/^{236}U_{RP}$ ratios from the RP release. The results show that the transit times of Atlantic water reached SEGC, SWGC and NWGC are 16 ± 2, 22 ± 2 and 22 ± 2 years (R^2 = 0.73, 0.75 and 0.77, respectively) from SF (Fig. S3, Table S2). For NEGC, although correlation analysis was not possible due to limited dataset, the observed $^{99}Tc/^{236}U_{RP}$ atomic ratios appear to match well with the two peaks in 1995 and 2002 in the discharge ratios based on visual estimation, indicating a 17 years transit time (Fig. 4D). These transport time estimates agree with previous estimates based the combination of ^{129}I and ^{236}U (17–22 years) in the west Fram Strait in northeastern Greenland (Wefing et al., 2021). Our findings also confirm that the water transport from east to northwest Greenland takes 5–6 years (Dahlgaard, 1995a; Hou et al., 2000).

An anticyclonic coastal current circulates around Iceland (Logenmann et al., 2013), with a branch of East Greenland Current from the NEGC transports south-eastward along the ridge of Iceland- Faroe Islands (Logenmann et al., 2013; Casanova-Masjoan et al., 2020). This branch of East Greenland Current may entrain RP signal to the southern coast of Iceland through Iceland Coastal Current and further return to SEGC. The mean $^{99}Tc/^{236}U_{RP}$ atomic ratio in 2019 Iceland costal water is comparable with that in Faroe Islands water in 2019, possibly indicating a similar Atlantic water transit time between Faroe Islands and Iceland. However, the dataset limits the application of correlation analysis in the coast of Faroe Islands and Iceland, so the mean $^{99}Tc/^{236}U_{RP}$ atomic ratios are also directly compared to historic RP discharge ratios. Our observation of mean $^{99}Tc/^{236}U_{RP}$ atomic ratios in the coast of Faroe Islands during 2017–2019

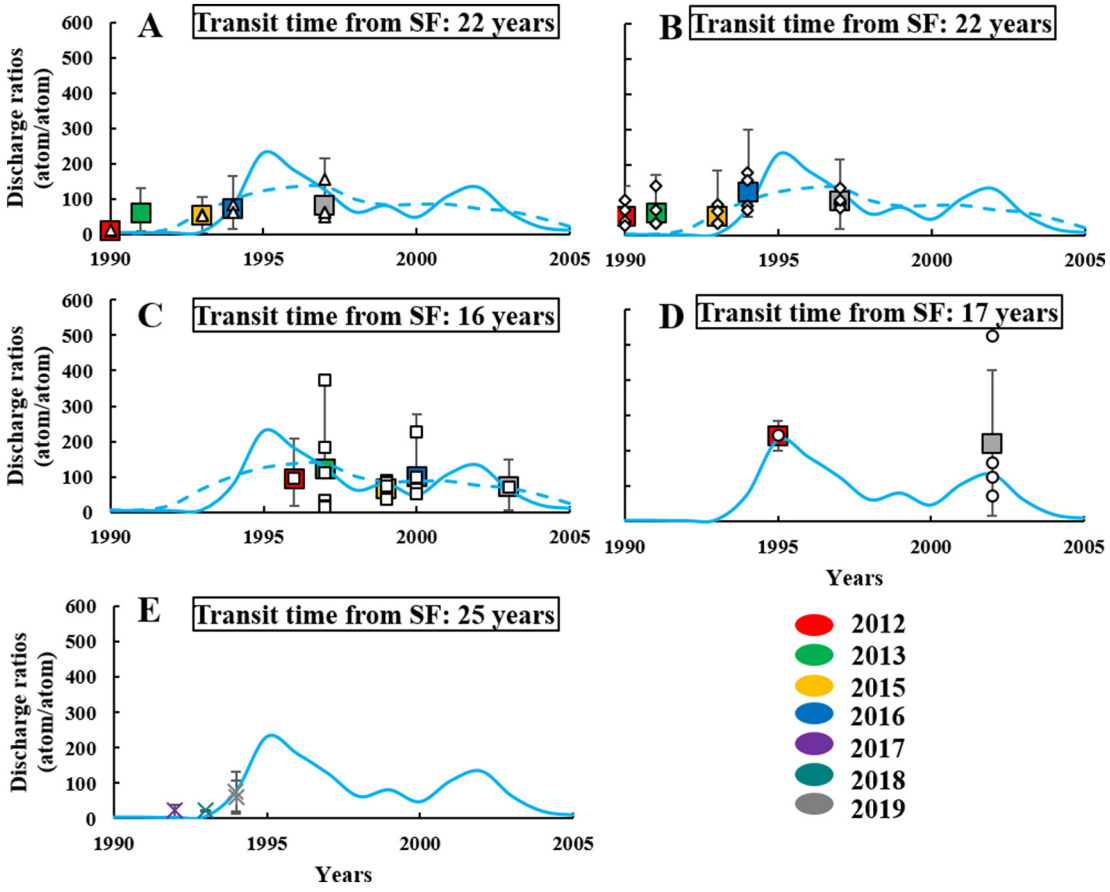

Fig. 4. The distribution of $^{99}Tc/^{236}U_{RP}$ atomic ratios in the NWGC (A), SWGC (B), SEGC (C), NEGC (D), IC and FIC (E) during 2012–2019. The temporal change of 5-year running average (dashed) and annual (solid) $^{99}Tc/^{236}U_{RP}$ atomic ratios from RP discharge is shown as a blue line. The colored boxes are the mean values of $^{99}Tc/^{236}U_{RP}$ ratios in seawater samples, where the colour depends on the year. The smaller symbols are individual observations. NWGC: north-western Greenland coast; SWGC: south-western Greenland coast; SEGC: south-eastern Greenland coast; NEGC: north-eastern Greenland coast; IC: Iceland coast; FIC: Faroe Islands coast.

shows an increasing trend with time, which appears to match well with the trend of discharge ratios in the period during 1992–1994 (Fig. 4). Thereby Atlantic water transit times from SF to Faroe Islands and Iceland are roughly estimated to be both 25 years.

4.2. The potential reason of unexpected ^{236}U concentration in the region of Greenland and Faroe Island

Anthropogenic ^{236}U in seawater is solely derived from GF and RP. Among the observations of ^{236}U concentrations during 2012–2019, an extremely high value was obtained in SEGC in 2013 ($128.6 \pm 17.3 \times 10^6$ atom/L of ^{236}U, 92 % of RP contribution, $0.12 \pm 0.01 \times 10^{-2}$ of $^{233}U/^{236}U$) (Fig. 3C, Table S1). Similarly, measurements from the coastal waters of the Faroe Islands also show an extremely high ^{236}U concentration ($115.9 \pm 7.9 \times 10^6$ atom/L, December 2nd, 2019) with significant RP contribution (96 %, $^{233}U/^{236}U$: $0.05 \pm 0.01 \times 10^{-2}$) (Fig. S4A and B). Although the deposition of GF in the world is not homogenous, GF ^{236}U concentration in mid-high latitude region decreases to relatively low level (10×10^6 atom/L in the North Sea) (Christl et al., 2015), suggesting that the extremely high ^{236}U concentration in surface seawater is unlikely to be derived from GF.

Generally, RP-derived ^{236}U in Greenland coast water derives from the outflowing polar water of the Arctic Ocean (Wefing et al., 2019; Qiao et al., 2020a). Previous studies also show that the current circulation pattern in the North Atlantic Ocean and the Arctic Ocean facilitates the transport of RP-derived ^{236}U with relatively higher level, but ^{236}U concentration is significantly diluted (10^6–10^7 atom/L) during the transport in the Arctic Ocean (Casacuberta et al., 2014, 2016, 2018; Wefing et al., 2021).

The high concentrations of ^{236}U are comparable to levels in LH branch water (10^8 atom/L in 2010) and the reconstructed ^{236}U concentration in SF branch water ($2.8–3.2 \times 10^8$ atom/L during 2012–2018) (Christl et al., 2017; Castrillejo et al., 2020). This indicates that an additional RP signal may be transported northwestwards from northern Europe without first entering the Arctic Ocean.

The unexpectedly high RP signal is also supported by other anthropogenic radioisotopes (^{90}Sr and ^{137}Cs). For instance, according to time-series monitoring data, $^{137}Cs/^{90}Sr$ activity ratios of 1.03–6.92 in Faroe Island coastal water appeared in 1990s (Fig. S4D) (AMAP 2010). A typical $^{137}Cs/^{90}Sr$ ratio for GF is approximately 1.5, as measured in seawater from the North Atlantic Ocean (Dahlgaard et al., 1995b). RP release results in much higher values. Considering the long residence time (~ 16 years) of ^{137}Cs, the sub-tidal sediments of Irish Sea are a continuous source of ^{137}Cs (Jenkinson et al., 2014), resulting in consistently high $^{137}Cs/^{90}Sr$ ratios in the ambient seawater in 1990s. The cumulative discharges from SF indicate $^{137}Cs/^{90}Sr$ activity ratios of 6.43–6.55 during 1991–1999 (OSPAR, 2019). Since GF was prevailing source for ^{137}Cs and ^{90}Sr in Faroe Islands coastal water, higher $^{137}Cs/^{90}Sr$ activity ratios in 1992 (4.36 ± 0.76) and 1997 (6.92 ± 0.34) reveal the existence of RP signal from SF (Fig. S4D). Combined this implies that there must be, at least sporadic, more direct connectivity between the waters leaving the North Sea and the SEGC. All these facts from anthropogenic radioisotopes suggest the sporadic connectivity of Faroe Island and Greenland coastal waters to the seawater in the western European coast, which could potentially explain the unexpected ^{236}U concentrations in Greenland and Faroe Islands coastal water (Fig. S4).

4.3. Perspectives

Anthropogenic radioisotopes with long half-lives (such as ^{99}Tc, ^{233}U and ^{236}U) offer a unique tool to study ocean currents and transit times. This is due to the combination of well-defined point sources (i.e., RP), high sensitivity of measurement (counting atoms per L), transient discharges ratios (time-dependent variations) and great specificity of sources (isotopic ratios). The major hurdle is the large sample volume (especially the case for ^{99}Tc) required a laborious sample preparation procedure. Further improvement of measurement techniques thus reducing sample volume requirements e.g., advanced AMS measurement for ^{99}Tc using ≤10 L of seawater (Hain et al., 2022), may permit the future use of tracking dispersion of RP signal further into the Atlantic and Arctic, and potentially into deep waters.

The ^{99}Tc-^{233}U-^{236}U approach tested here holds potential as it can easily isolate the RP signal, separating the contribution to ^{236}U from GF. The ubiquitous GF contribution may introduce uncertainties in estimating transit times of Atlantic water. Downstream, far from reprocessing plants, such as in the Arctic, the GF contribution continuously increases with water transport, and additional inputs from GF in Siberian catchments and glacial meltwater may play a greater role. The testing of the approach in the subarctic and Arctic Atlantic, near to point sources indicates that it gives similar transit times to that from $^{129}I/^{236}U$, confirming that GF interference since 1990s is not significant for estimating Atlantic water transit time in these waters. Finally due to the extreme specificity of the radiotracer approach, these measurements can offer the only empirical evidence of connectivity across ocean basins, which can be used to verify ocean circulation modelling and indicate new dispersion pathways for contaminants and organisms.

5. Conclusion

In this work, we report the first application to estimate the Atlantic water transit time in the Greenland coast based on a purely RP-derived dual-tracer ($^{99}Tc/^{236}U_{RP}$ transformed from ^{99}Tc-^{233}U-^{236}U). The estimated range of Atlantic water transit time in the Greenland coast (16–22 years) supports earlier estimates using different radioisotopes from samples in the western Fram Strait of the northeastern Greenland coast. The transit times of Atlantic water from northern Europe to both Iceland and Faroe Islands are estimated to be 25 years. The proposed radiotracer approach isolated the RP signal thus excludes the interference from the ubiquitous GF signal. This method provides independent validation to the existing ^{129}I—^{236}U tracer approach where GF ^{236}U was not isolated. The ^{99}Tc-^{233}U-^{236}U radiotracer approach is expected to be robust in estimating Atlantic water transit times in the North Atlantic-Arctic region. With the continuous transport of outflowing polar water, the use of long-lived ^{99}Tc-^{233}U-^{236}U is a potential tool to trace the outflowing water in a large-scale region, such as the tropical Atlantic Ocean and the South Atlantic Ocean.

Supplementary data to this article can be found online at https://doi.org/10.1016/j.scitotenv.2022.158276.

CRediT authorship contribution statement

Gang Lin: Conceptualization, Data curation, Formal analysis, Investigation, Methodology, Writing – original draft. **Jixin Qiao:** Conceptualization, Data curation, Formal analysis, Funding acquisition, Investigation, Methodology, Resources, Supervision, Writing – review & editing. **Peter Steier:** Data curation, Investigation, Methodology, Resources. **Magnús Danielsen:** Investigation, Resources. **Kjartan Guðnason:** Investigation, Resources. **Hans Pauli Joensen:** Investigation, Resources. **Colin A. Stedmon:** Conceptualization, Formal analysis, Investigation, Methodology, Supervision, Writing – review & editing.

Declaration of competing interest

The authors declare that they have no known competing financial interests or personal relationships that could have appeared to influence the work reported in this paper.

Acknowledgements

We thank employees at National Institute of Aquatic Resources, Denmark, Marine and Freshwater Research Institute, Iceland, and University of Faroe Islands for the help in seawater samples collection. This study was supported by the Independent Research Fund Denmark (9040-00266B). J. Qiao wishes to thank the 'Radioactivity, AMAP 2018-2019'

project (J. nr. MST-113-00080) and 'Radioactivity, AMAP-2015' project (J. nr. MST-112-00223) granted by Environmental Protection Agency, Danish Ministry of the Environment for financial support. The RADIATE project (21002412-ST) from the EU Research and Innovation programme HORIZON 2020 under grant agreement No 824096 supports part of the AMS measurements.

References

Aarkrog, A., Boelskifthe, S., Dahlgaard, H., Duniec, S., Hallstadius, L., Holm, E., Smith, J.N., 1987. Technetium-99 and Caesium-134 as long distance tracers in Arctic water. Estuar. Coast. Shelf Sci. 24, 637–647. https://doi.org/10.1016/0272-7714(87)90103-X.

Carscadden, J.E., Gjøsæter, H., Vilhjálmsson, H., 2013. A comparison of recent changes in distribution of capelin (Mallotus villosus) in the Barents Sea, around Iceland and in the Northwest Atlantic. Prog. Oceanogr. 114, 64–83. https://doi.org/10.1016/j.pocean.2013.05.005.

Casacuberta, N., Christl, M., Lachner, J., van der Loeff, M.R., Masqué, P., Synal, H.-A., 2014. A first transect of 236U in the North Atlantic Ocean. Geochim. Cosmochim. Acta 133, 34–46. https://doi.org/10.1016/j.gca.2014.02.012.

Casacuberta, N., Masqué, P., Henderson, G., van-der-Loeff, M.R., Bauch, D., Vockenhuber, C., Daraoui, A., Walther, C., Synal, H.A., Christl, M., 2016. First 236U data from the Arctic Ocean and use of 236U/238U and 129I/236U as a new dual tracer. Earth Planet. Sci. Lett. 440, 127–134. https://doi.org/10.1016/j.epsl.2016.02.020.

Casacuberta, N., Christl, M., Vockenhuber, C., Wefing, A.-M., Wacker, L., Masqué, P., Synal, H.-A., van der Loeff, M.R., 2018. Tracing the three Atlantic branches entering the Arctic Ocean with 129I and 236U. J. Geophys. Res. Oceans 123, 6909–6921. https://doi.org/10.1029/2018JC014168.

Casanova-Masjoan, M., Pérez-Hernández, M.D., Pickart, R.S., Valdimarsson, H., Ólafsdóttir, S.R., Macrander, A., et al., 2020. Along-stream, seasonal, and interannual variability of the North Icelandic Irminger Current and East Icelandic Current around Iceland. J. Geophys. Res. Oceans 125, e2020JC016283. https://doi.org/10.1029/2020JC016283.

Castrillejo, M., Witbaard, R., Casacuberta, N., Richardson, C.A., Dekker, R., Synal, H.-A., Christl, M., 2020. Unravelling 5 decades of anthropogenic 236U discharge from nuclear reprocessing plants. Sci. Total Environ. 717 (137094), 2020. https://doi.org/10.1016/j.scitotenv.2020.137094.

Chamizo, E., Christl, M., López-Lora, M., Casacuberta, N., Wefing, A.-M., Kenna, T.C., 2022. The potential of 233U/236U as a water mass tracer in the Arctic Ocean. J. Geophys. Res. Oceans 127, e2021JC017790. https://doi.org/10.1029/2021JC017790.

Chen, Q., Dahlgaard, H., Nielsen, S.P., 1994. Determination of 99Tc in sea water at ultra low levels. Anal. Chim. Acta 285, 177–180. https://doi.org/10.1016/0003-2670(94)85021-6.

Chen, Q., Hou, X., Yu, Y., Dahlgaard, H., Nielsen, S.P., 2002. Separation of Sr from Ca, Ba and Ra by means of Ca(OH)2 and Ba(Ra)Cl2 or Ba(Ra)SO4 for the determination of radiostrontium. Anal. Chim. Acta 466, 109–116. https://doi.org/10.1016/S0003-2670(02)00571-8.

Christl, M., Lachner, J., Vockenhuber, C., Lechtenfeld, O., Stimac, I., van der Loeff, M.R., Synal, H.-A., 2012. A depth profile of uranium-236 in the Atlantic Ocean. Geochim. Cosmochim. Acta 77, 98–107. https://doi.org/10.1016/j.gca.2011.11.009.

Christl, M., Casacuberta, N., Vockenhuber, C., Elsässer, C., Bailly du Bois, P., Herrmann, J., Synal, H.A., 2015. Reconstruction of the 236U input function for the Northeast Atlantic Ocean: implications for 129I/236U and 236U/238U-based tracer ages. Journal of Geophysical Research: Oceans 120, 7282–7299. https://doi.org/10.1002/2015JC011116.

Christl, M., Casacuberta, N., Lachner, J., Herrmann, J., Synal, H.-A., 2017. Anthropogenic 236U in the North Sea – a closer look into a source region. Environ. Sci. Technol. 51, 12146–12153. https://doi.org/10.1021/acs.est.7b03168.

Dahlgaard, H., 1994. Source of 137Cs, 90Sr and 99Tc in the East Greenland Current. J. Environ. Radioact. 25, 37–55. https://doi.org/10.1016/0265-931X(94)90006-X.

Dahlgaard, H., 1995a. Transfer of European coastal pollution to the arctic: radioactive tracers. Mar. Pollut. Bull. 31, 3–7. https://doi.org/10.1016/0025-326X(95)00003-6.

Dahlgaard, H., Chen, Q., Herrmann, J., Nies, H., Ibbett, R.D., Kershaw, P.J., 1995b. On the background level of 99Tc, 90Sr and 137Cs in the North Atlantic. J. Mar. Syst. 6, 571–578. https://doi.org/10.1016/0924-7963(95)00025-K.

Daniault, N., Mercier, H., Lherminier, P., Sarafanov, A., Falina, A., Zunino, P., et al., 2016. The northern North Atlantic Ocean mean circulation in the early 21st century. Prog. Oceanogr. 146, 142–158. https://doi.org/10.1016/j.pocean.2016.06.007.

Hain, K., Steier, P., Froehlich, M.B., Golser, R., Hou, X., Lachner, J., Qiao, J., Quinto, F., Sakaguchi, A., 2020. 233U/236U signature allows to distinguish environmental emissions of civil nuclear industry from weapons fallout. Nat. Commun. 11. https://doi.org/10.1038/s41467-020-15008-2.

Hain, K., Martschini, M., Gülce, F., Honda, M., Lachner, J., Kern, M., Pitters, J., Quinto, F., Sakaguchi, A., Steier, P., Wiederin, A., 2022. Developing accelerator mass spectrometry capabilities for anthropogenic radionuclide analysis to extend the set of oceanographic tracers. Front. Mar. Sci. 9, 837515. https://doi.org/10.3389/fmars.2022.837515.

Halloran, P.R., Hall, I.R., Menary, M., Reynolds, D.J., Scourse, J.D., Screen, J.A., et al., 2020. Natural drivers of multidecadal Arctic sea ice variability over the last millennium. Sci. Rep. 10 (668), 1–9. https://doi.org/10.1038/s41598-020-57472-2.

Hátún, H., Lohmann, K., Matei, D., Jungclaus, J., Pacariz, S., Bersch, M., Gislason, A., Ólafsson, J., Reid, P.C., 2016. An inflated subpolar gyre blows life towards the northeastern Atlantic. Prog. Oceanogr. 147, 49–66. https://doi.org/10.1016/j.pocean.2016.07.009.

Hátún, H., Azetsu-Scott, K., Somavilla, R., Rey, F., Johnson, C., Mathis, M., Mikolajewicz, U., Coupel, P., Tremblay, J.-É., Hartman, S., Pacariz, S.V., Salter, I., Ólafsson, J., 2017. The subpolar gyre regulates silicate concentrations in the North Atlantic. Sci. Rep. 7, 14576. https://doi.org/10.1038/s41598-017-14837-4.

Hou, X.L., Dahlgaard, H., Nielsen, S.P., 2000. Iodine-129 time series in Danish, Norwegian and northwest Greenland coast and the Baltic Sea by seaweed. Estuar. Coast. Shelf Sci. 51, 571–584. https://doi.org/10.1006/ecss.2000.0698.

International Atomic Energy Agency (IAEA), 2004. Sediment distribution coefficients and concentration factors for biota in the marine environment. Technical Reports Series No. 422 9–25.

Jackson, D., 2000. Related content radiation doses to members of the public near to Sellafield, Cumbria, from liquid discharges 1952-. J. Radiol. Prot. 20, 139–167.

Jenkinson, S.B., McCubbin, D., Kennedy, P.H.W., Dewar, A., Bonfield, R., Leonard, K.S., 2014. An estimate of the inventory of technetium-99 in the sub-tidal sediments of the Irish Sea. J. Environ. Radioact. 133, 40–47. https://doi.org/10.1016/j.jenvrad.2013.05.004.

Karcher, M.J., Gerland, S., Harms, I.H., Iosjpe, M., Heldal, H.E., Kershaw, P.J., Sickel, M., 2004. The dispersion of 99Tc in the Nordic Seas and the Arctic Ocean: a comparison of model results and observations. Journal of Environmental Radioactivity 74, 185–198. https://doi.org/10.1016/j.jenvrad.2004.01.026.

Kershaw, P.J., McCubbin, D., Leonard, K.S., 1999. Continuing contamination of North Atlantic and Arctic waters by sellafield radionuclides. Sci. Total Environ. 237 (238), 119–132. https://doi.org/10.1016/S0048-9697(99)00129-1.

Lin, M., Qiao, J.X., Hou, X.L., Golser, R., Hain, K., Steier, P., 2021a. On the quality control for the determination of ultratrace-level 236U and 233U in environmental samples by accelerator mass spectrometry. Anal. Chem. 93, 3362–3369. https://doi.org/10.1021/acs.analchem.0c03623.

Lin, M., Qiao, J., Hou, X., Dellwig, O., Steier, P., Hain, K., Golser, R., Zhu, L., 2021b. 70-year anthropogenic uranium imprints of nuclear activities in Baltic Sea sediments. Environ. Sci. Technol. 55 (13), 8918–8927. https://doi.org/10.1021/acs.est.1c02136.

Logenmann, K., Ólafsson, J., Snorrason, Á., Valdimarsson, H., Marteinsdóttir, G., 2013. The circulation of icelandic waters – a modelling study. Ocean Sci. 9, 931–955. https://doi.org/10.5194/os-9-931-2013.

Muilwijk, M., Smedsrud, L.H., Ilicak, M., Drange, H., 2018. Atlantic water heat transport variability in the 20th century Arctic Ocean from a global ocean model and observations. J. Geophys. Res. Oceans 123, 8159–8179. https://doi.org/10.1029/2018JC014327.

OSPAR, 2019. Liquid Discharges from Nuclear Installations [WWW Document]. https://www.ospar.org.

Periáñez, R., Suh, K.S., Min, B.I., Villa-Alfageme, M., 2018. The behaviour of 236U in the North Atlantic Ocean assessed from numerical modelling: a new evaluation of the input function into the Arctic. Sci. Total Environ. 626, 255–263. https://doi.org/10.1016/j.scitotenv.2018.01.058.

Polyakov, I.V., Pnyushkov, A.V., Alkire, M.B., Ashik, I.M., Baumann, T.M., Carmack, E.C., Goszczko, I., Guthrie, J., Ivanov, V.V., Kanzow, T., Krishfield, R., Kwok, R., Sundfjord, A., Morison, J., Rember, R., Yulin, A., 2017. Greater role for Atlantic inflows on sea ice loss in the Eurasian Basin of the Arctic Ocean. Science 356 (6335), 285–291. https://doi.org/10.1126/science.aai8204.

Qiao, J.X., Xu, Y.H., 2018. Direct measurement of uranium in seawater by inductively coupled plasma mass spectrometry. Talanta 183, 18–23. https://doi.org/10.1016/j.talanta.2018.02.045.

Qiao, J.X., Hou, X.L., Steier, P., Nielsen, S., Golser, R., 2015. Method for 236U determination in seawater using flow injection extraction chromatography and accelerator mass spectrometry. Anal. Chem. 87, 7411–7417. https://doi.org/10.1021/acs.analchem.5b01608.

Qiao, J.X., Hain, K., Steier, P., 2020a. First dataset of 236U and 233U around the Greenland coast: a 5-year snapshot (2012–2016). Chemosphere 257, 127185. https://doi.org/10.1016/j.chemosphere.2020.127185.

Qiao, J.X., Andersson, K., Nielsen, S., 2020b. A 40-year marine record of 137Cs and 99Tc transported into the Danish Straits: significance for oceanic tracer studies. Chemosphere 244, 125595. https://doi.org/10.1016/j.chemosphere.2019.125595.

Qiao, J., Ransby, D., Steier, P., 2022. Deciphering anthropogenic uranium sources in the equatorial northwest Pacific margin. Sci. Total Environ. 806, 150482. https://doi.org/10.1016/j.scitotenv.2021.150482.

Rozmaric, M., Chamizo, E., Louw, D.C., López-Lora, M., Blinova, O., Levy, I., Mudumbi, B., van der Plas, A.K., Tenorio, R.G., McGinnity, P., Osvath, I., 2022. Fate of anthropogenic radionuclides (90Sr, 137Cs, 238Pu, 239Pu, 240Pu, 241Am) in seawater in the northern Benguela upwelling system off Namibia. Chemosphere 286, 131514. https://doi.org/10.1016/j.chemosphere.2021.131514.

Sakaguchi, A., Kawai, K., Steier, P., Quinto, F., Mino, K., Tomita, J., Hoshi, M., Whitehead, N., Yamamoto, M., 2009. First results on 236U levels in global fallout. Sci. Total Environ. 407, 4238–4242. https://doi.org/10.1016/j.scitotenv.2009.01.058.

Sakaguchi, A., Kadokura, A., Steier, P., Takahashi, Y., Shizuma, K., Hoshi, M., Nakakuki, T., Yamamoto, M., 2012. Uranium-236 as a new oceanic tracer: a first depth profile in the Japan Sea and comparison with caesium-137. Earth Planet. Sci. Lett. 333, 165–170. https://doi.org/10.1016/j.epsl.2012.04.004.

Shi, K., Hou, X., Roos, P., Wu, W., 2012. Determination of technetium-99 in environmental samples: a review. Anal. Chim. Acta 709, 1–20. https://doi.org/10.1016/j.aca.2011.10.020.

Smith, J.N., McLaughlin, F.A., Smethie, W.M., Moran, S.B., Lepore, K., 2011. Iodine-129, 137Cs, and CFC-11 tracer transit time distributions in the Arctic Ocean. J. Geophys. Res. 116, C04024. https://doi.org/10.1029/2010JC006471.

Smith, J.N., Karcher, M., Casacuberta, N., Williams, W.J., Kenna, T., Smethie Jr., W.M., 2021. A changing Arctic Ocean: how measured and modeled 129I distributions indicate fundamental shifts in circulation between 1994 and 2015. J. Geophys. Res. Oceans 126, e2020JC016740. https://doi.org/10.1029/2020JC016740.

Steier, P., Bichler, M., Keith Fifield, L., Golser, R., Kutschera, W., Priller, A., Quinto, F., Richter, S., Srncik, M., Terrasi, P., Wacker, L., Wallner, A., Wallner, G., Wilcken, K.M., Maria Wild, E., 2008. Natural and anthropogenic 236U in environmental samples. Nucl. Inst. Methods Phys. Res. B 266, 2246–2250. https://doi.org/10.1016/j.nimb.2008.03.002.

Steier, P., Dellinger, F., Forstner, O., Golser, R., Knie, K., Kutschera, W., Priller, A., Quinto, F., Srncik, M., Terrasi, F., Vockenhuber, C., Wallner, A., Wallner, G., Wild, E.M., 2010. Analysis and application of heavy isotopes in the environment. Nucl. Inst. Methods Phys. Res. B 268 (7–8), 1045–1049. https://doi.org/10.1016/j.nimb.2009.10.094.

Wefing, A.-M., Christl, M., Vockenhuber, C., Rutgers van der Loeff, M., Casacuberta, N., 2019. Tracing Atlantic waters using 129I and 236U in the Fram Strait in 2016. J. Geophys. Res. Oceans 124, 882–896. https://doi.org/10.1029/2018JC014399.

Wefing, A.-M., Casacuberta, N., Christl, M., Gruber, N., Smith, J.N., 2021. Circulation timescales of Atlantic water in the Arctic Ocean determined from anthropogenic radionuclides. Ocean Sci. 17, 111–129. https://doi.org/10.5194/os-17-111-2021.